Spanwise Rotation and Wall Curvature Effects on Instability of Boundary Layer

Koji Kikuyama, professor
Yutaka Hasegawa, associate professor
Noboru Matsumoto, graduate student
Michio Nishikawa, graduate student
Department of Mechanical Engineering, Nagoya University
Chikusa-ku, Nagoya Japan 464 4703

Abstract

The behavior of the boundary layer flows in rotating channels such as impeller passages of turbomachinery are dominated by the centrifugal and Coriolis forces due to the wall curvature and system rotation, respectively, which predominate the boundary layer development by suppressing or promoting the turbulent motion. Though many studies have been made about the turbulent boundary layer over a concave or convex surface in the stationary state, the resultant effects due to the Coriolis force in the rotational frame of reference have scarcely been researched.

In the present study the velocity and turbulent intensity are measured near the concave surface in channels whose radii of center line curvature are 1,000mm and 2,000mm, respectively, on the rotating system.

When the channel rotates in such direction as the Coriolis force acts toward the wall, the transition of the boundary layer to the turbulent state is promoted because the Görtler instability is enhanced but it is suppressed when the force acts in the opposite direction.

1. Introduction

Prediction of turbomachinery performance needs the detailed knowledge of flow patterns inside and at the exit of impeller passages, and to examine the effects of the rotation and curvature of the channel, some studies have been made on each of these subjects.

The turbulent motion is known to be suppressed near the convex surface and promoted near the concave one due to the centrifugal force, and Bradshaw(1969) showed a similar relationship between the centrifugal force in a curved channel and the Coriolis force in a rotating straight channel. In rotating straight channels, Johnston(1973) and Koyama et al.(1979) examined the stability effects of the Coriolis force by experiments. Using a curved channel, the present authors(1987) clarified experimentally the resultant effects of the centrifugal and Coriolis forces upon the turbulent boundary layer near the concave and convex surfaces of the channel.

For a laminar boundary layer, Matsson and Alfredsson(1990) made experiments about the effects of the channel rotation on the occurrence of longitudinal vortices and Matsubara et al.(1991) made a series of experiments on the instability effects of the Coriolis force upon a laminar boundary layer on a rotating flat plate.

The present authors(1994,2000) have performed calculation for the instability of a laminar boundary layer near the curved rotating wall and showed that the Coriolis force contributes to the occurrence of the Görtler vortices. The Coriolis force, however, is found to suppress T-S instability in the pressure side but to promote it in the suction side.

Despite these numerical studies, there are few experimental studies on the boundary layer flows along a carved surface in the rotating channel. This paper represents the experimental results on the distributions of velocity and fluctuating components, and discusses the transition of laminar boundary layer for different rotational speeds and two different curvature radii of the wall.

2. Equipment and Method of Experiment

Figure 1 shows the schematic outline of the experimental equipment. Air was introduced through a two-dimensional nozzle, into the curved channel and exhausted to the atmosphere through the rotating axis by a blower settled in the stationary system. The rotating table supported by thrust bearings can rotate both in the clockwise and anti-clockwise directions. Two channels of different radii of curvature, R = 1,000mm and 2,000mm were adopted for the experiment. Measurements of velocities were made by a hot-wire probe and pressure transducers, mounted on the rotating table, whose output signals were transmitted to the stationary system by means of slip rings.

Figure 2 shows the measurement sections of the channel with R = 1,000mm. In order to avoid the effects of the upstream boundary layer developing along the contraction nozzle on the test wall, a thin plate whose width is 10mm was inserted on the center line

Tab.1 Longitudinal distances of measurement sections, x/d, for channels of R = 1,000mm and 2,000mm (d = 50mm)

Section / R	O_1	O_2	O_3	O_4	O_5	O_6	O_7
1000mm	2.60	8.21	16.02	23.84	31.65	39.47	47.28
2000mm	2.80	7.73	15.56	23.40	31.23	36.16	

TOP VIEW

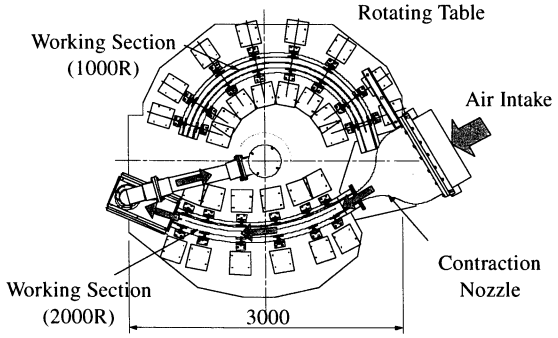

SIDE VIEW

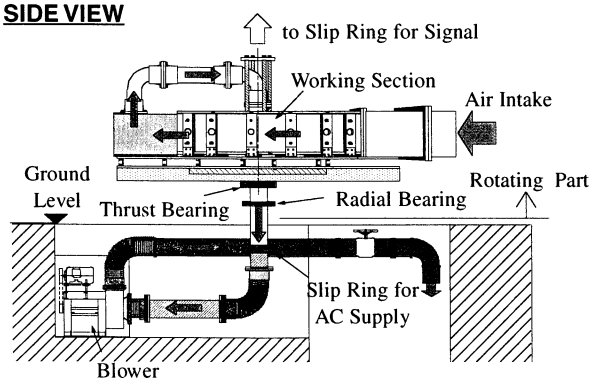

Fig.1 Schematic outline of experimental equipment [in mm]

of the channel and uniform flow was ascertained to be introduced into the concave side of the plate. The longitudinal distances of the measuring sections from the leading edge of the plate are listed in Tab. 1 for the two channels of R = 1,000 and 2,000mm.

Figure 3 shows the configuration of a measurement section. The aspect ratio h/d is 8:1 to get rid of the effects from the end walls and the probe was traversed at the mid-height of the section as shown by a line B-B in the figure.

The Reynolds number based on the free stream velocity in the section O_1 and the channel width, $Re = U_m d/\nu$, was taken to be 1.8 and 3.6 x 10^4, respectively and the dimensionless rotation rate, N, defined by the following relation was taken to be 0, $\pm$ 0.012, where the sign of N denotes the difference in the rotational direction of channels and its positive value corresponds

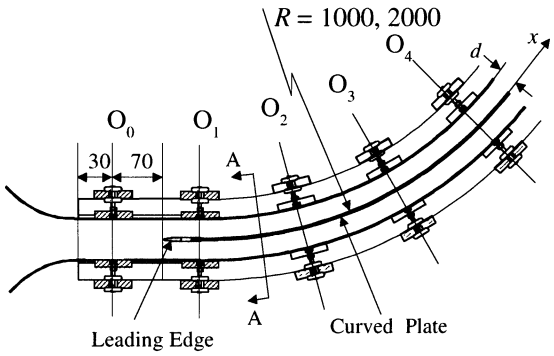

Fig.2 Measurement sections in curved channel [in mm]

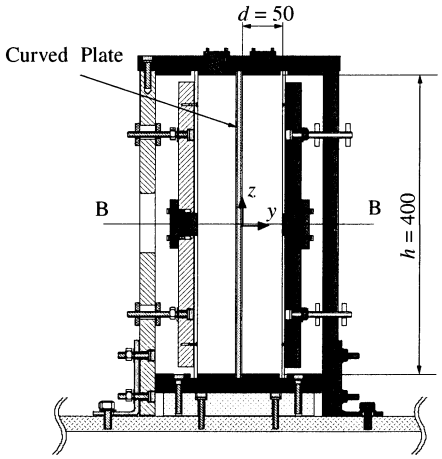

Fig.3 Configuration and dimensions of cross-section (A-A in Fig.2) [in mm]

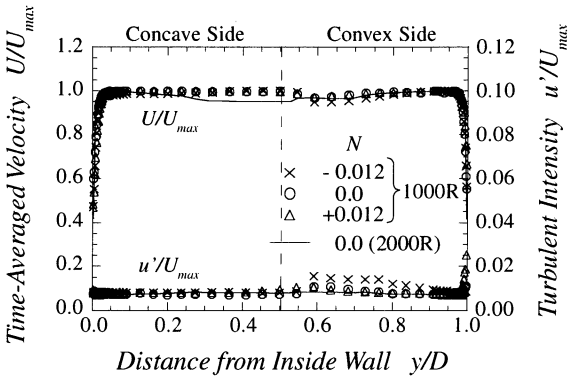

Fig.4 Distributions of time-mean and fluctuating components of velocity in section O_0, at the exit of nozzle [in mm]

to the direction of the Coriolis force acting toward the concave wall.

$$N = d\Omega/U_m \qquad (1)$$

3. Experimental Results and discussions

3.1 Inlet velocity

The velocity profiles in the section of O_0 just downstream of the inlet nozzle are plotted for different ro-

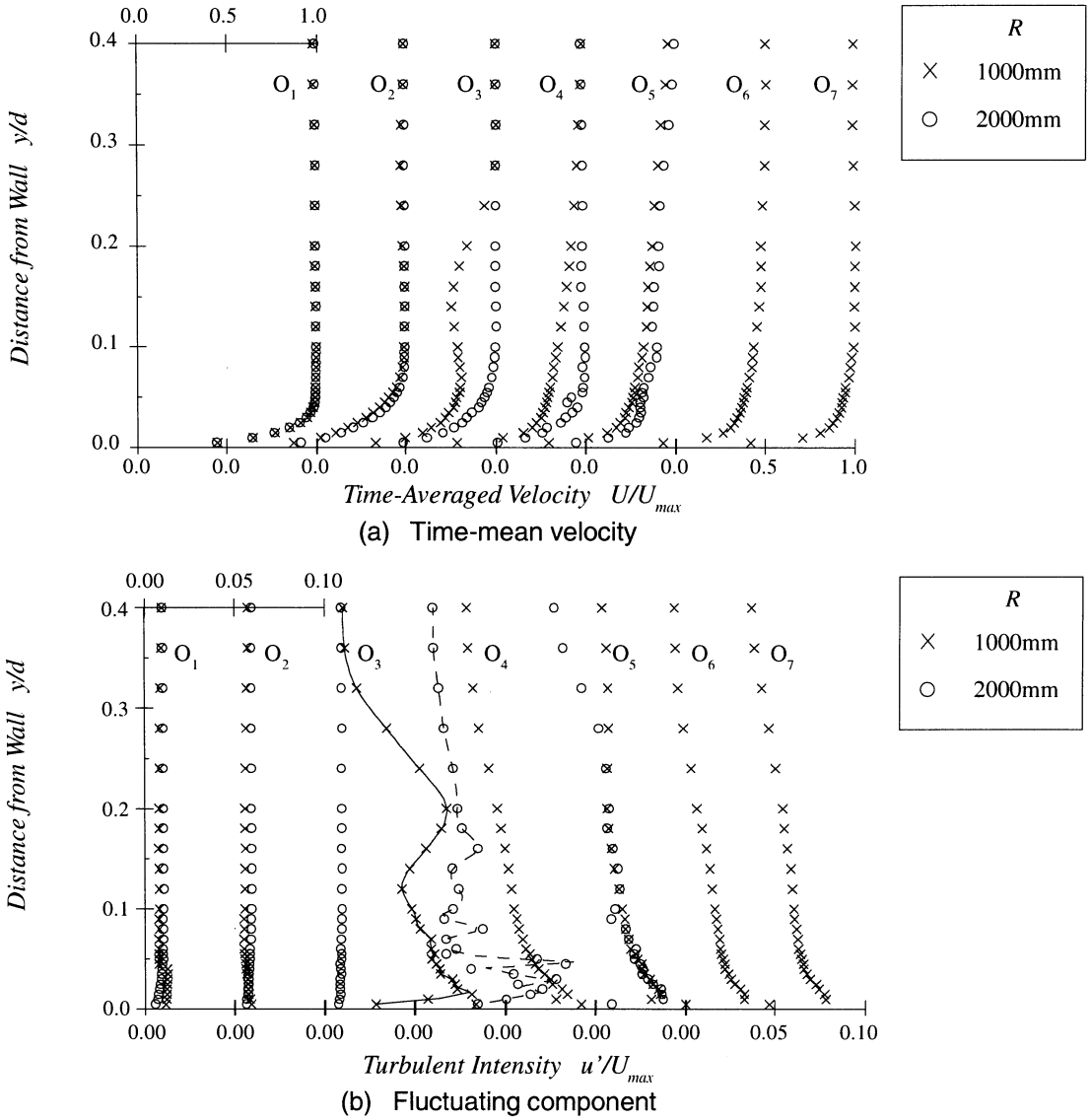

Fig. 5 Downstream change in time-mean and fluctuating components profile in the stationary state

tation rates in Fig.4, when the curved channel of R = 1,000mm is jointed with the nozzle. Few difference can be seen among the different rotation rates. Some disturbances in the time-mean velocity profile in the mid-region of the section may be considered due to the displacement effects of the inserted support of the hot-wire probe. In the same figure the profile for R = 2,000mm and N = 0 is plotted by a solid line. As the flow was split by a thin plate inserted along the center line of the channel just downstream of this section, a uniform flow with its fluctuating component of u'/Um being nearly 1% is introduced into the test section

3.2 Velocity and turbulent intensity distribution in stationary state

Since the centrifugal force affects the boundary layer development and the transition to turbulent state, the downstream change in the time-mean and fluctuating components are examined as shown in Fig.5(a) and

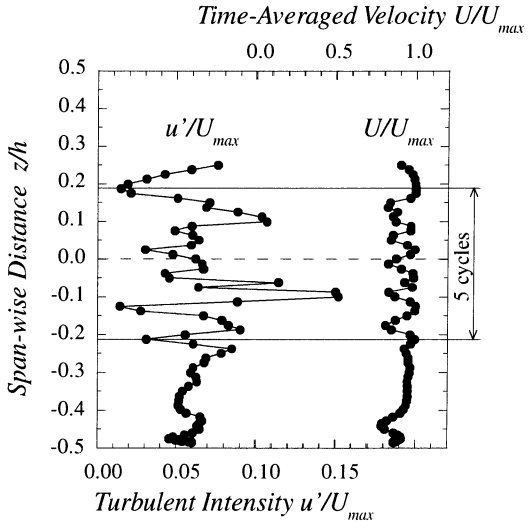

Fig.6 Lateral distributions of time-mean and fluctuating components of velocity at section O_3 of R = 2,000mm in the stationary state

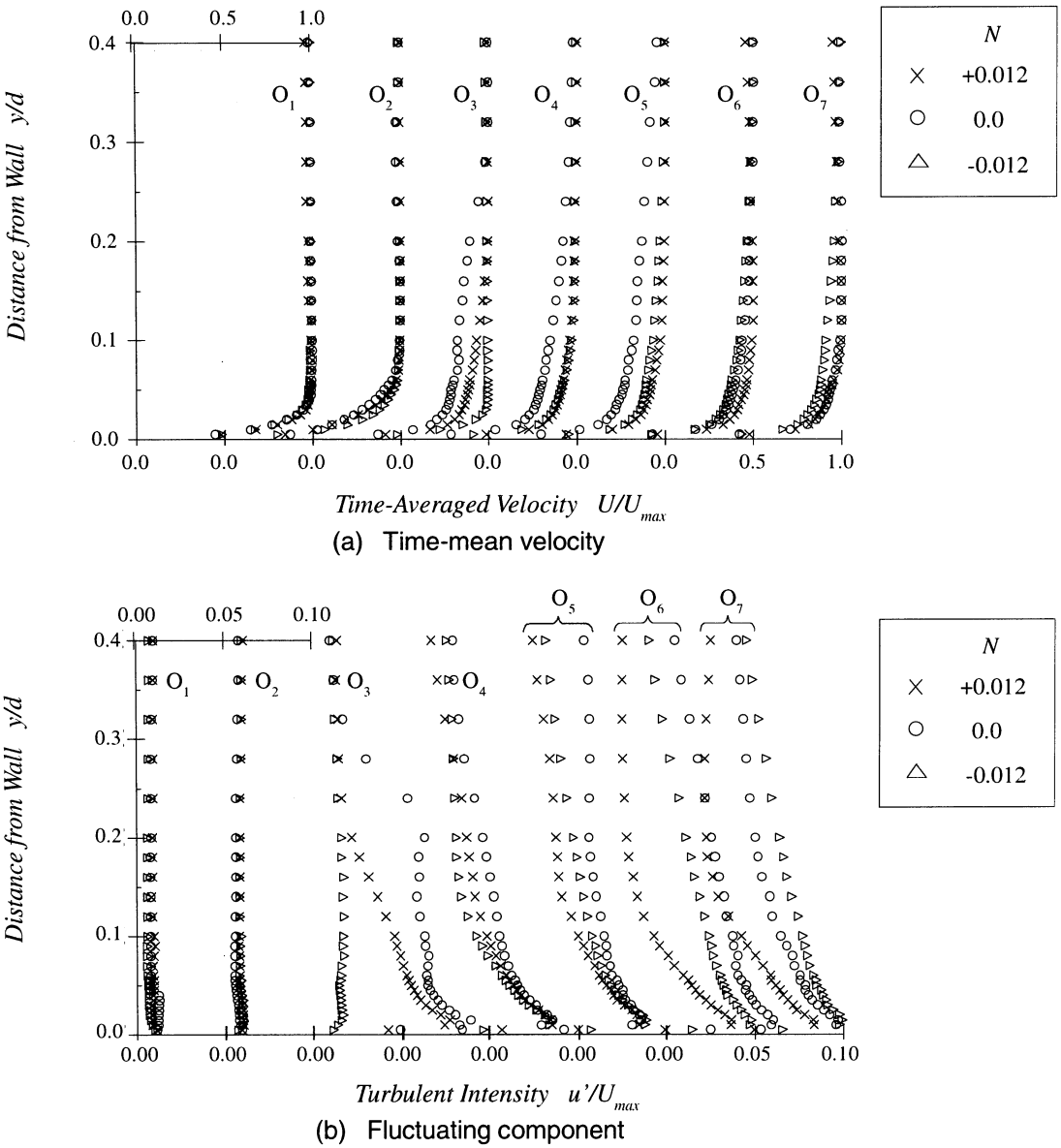

Fig.7 Longitudinal change in time-mean and fluctuating profile for R = 1,000mm at different rotation rates

(b) for the curvature radii of R =1,000 and 2,000mm, respectively. The flow is seen to remain in the laminar state as far as the section of O_2, but at the section O_3 in the channel of R = 1,000mm the profile exhibits a wavy type suggesting an occurrence of the Görtler instability caused by the centrifugal force and the flow is changed to a turbulent state in the downstream sections. The same phenomena can be seen in the channel of R = 2,000mm, but the occurrence the instability is delayed to the section of O_4 because of the smaller effect of the centrifugal force due to the streamline curvature.

In order to confirm the generation of the Görtler vortices along the concave wall, the hot-wire probe was traversed in z-direction, parallel to the wall surface at the distance of y/d = 0.1 in the section of O_4 of R = 2,000mm. Figure 6 shows the distributions of time-mean velocity and turbulence intensity, which suggest existence of stream-wise vortices, where the higher velocity corresponds to the lower fluctuation, and vice versa. The increase in the fluctuating component in the section O_4 shown in Fig.5(b) is considered to be due to this stream-wise vortices, which carries fluids with larger fluctuation near the wall toward the main stream.

3.3 Effects of rotation on the boundary layer flow along concave wall

As the channel rotates around the axis parallel to the spanwise direction of the concave wall, the boundary layer is subject to the Coriolis force acting toward or away from the wall according to the rotational direction. Figure 7(a) and (b) shows the longitudinal change

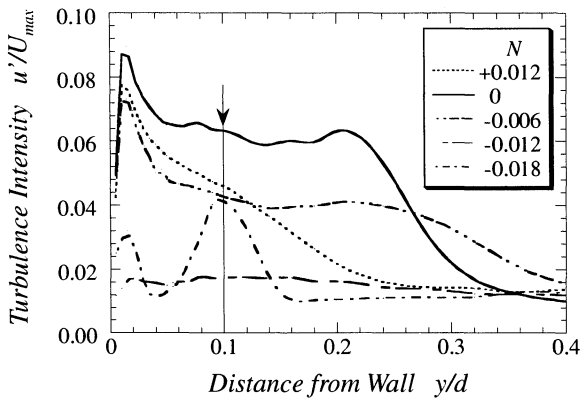

Fig.8 Distribution of fluctuating component at section O_3 for R = 1,000mm

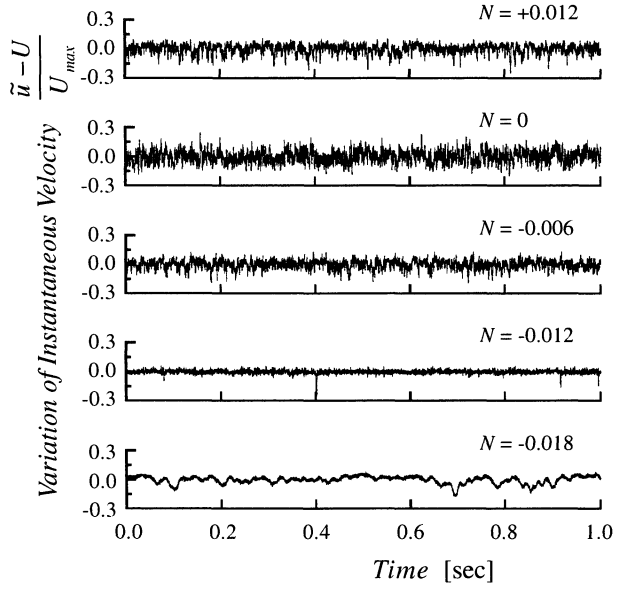

Fig.9 Output signal of fluctuating component at y/d = 0.1 of section O_3

in the velocity and turbulence intensity profiles in the channel of R = 1,000mm for N = 0, and $\pm$0.012. The positive value of N denotes that the Coriolis force acts in the same direction as the centrifugal one, resulting in the increase in the static pressure toward the wall. All the profiles in the section of O_2 are seen to be in the laminar state and they are changed into turbulent state at O_3 for the rotational condition of $N \geqq 0$, but remains laminar when N is equal to -0.012.

In further downstream sections the flow changes into turbulent state and the turbulent intensity is seen to be smaller in the boundary layer for the positive rotation rate. This can be attribute to a secondary flow which may be generated by the two forces and shift the lower fluctuating fluids toward the test wall in the midsection of the channel, at z/d = 0.

To examine further the effects of the channel rotation in the section of O_3, the fluctuating component is plotted for the rotation rates of 0.012, 0, -0.006, -0.012 and -0.018 in Fig 8. The flow is considered to be turbulent for N > -0.006, but fluctuation is suppressed when N is decreased to -0.012. Further decrease of N to -0.018 causes a different instability seen near y/d = 0.1. The time traces of the fluctuating component are shown in Fig.9 for the corresponding values of N. The dominant frequencies of the fluctuation for N = -0.018 is found to be lower than other rotation rates. Figure 10 shows the comparison of the power spectrum of the fluctuation for N = 0.012, 0 and -0.018. Compared with the curve of N = 0, which exhibits a turbulent flow nature, that for N = -0.018 has a dominant frequency of nearly 10Hz.

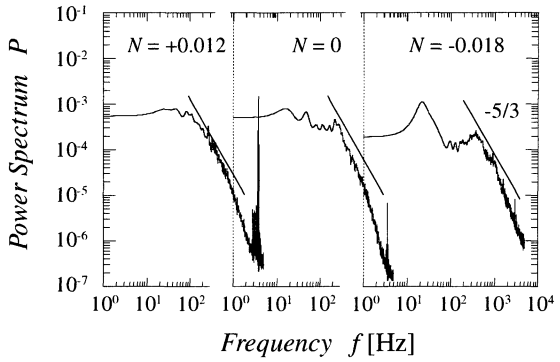

Fig.10 Power spectrum of fluctuating component

According to the previous calculations conducted by the present authors, the critical Görtler number, below which the Görtler vortices of any size cannot be generated, is increased and the generation of Görtler vortices are suppressed but the marginal stability curve in Re_θ-(wave number) plane enlarges, showing that the T-S instability is promoted when N is negative. Thus, for N = -0.018, the nature of the instability may differ from those prevailing for the conditions of positive N.

As the Coriolis force and centrifugal force were found to have a large effects on the development and transition of boundary layer, the change in the momentum thickness, θ, and shape parameter, H, in the channel of R = 2,000 are plotted in Fig. 11 (a) and (b), respectively.

From the curves of θ and H the transition into turbulent state is seen to be delayed by the Coriolis force when N is negative, but enhanced when N is positive. Though the transition occurs at the Reynolds number of $Re_{x_{cr}}$ of about 10^6 for the boundary layer on a stationary flat plate, Fig. 11(a) and (b) shows that the transition is advanced for all rotational conditions due to higher turbulence level in the inlet flow and occurs at different values of $Re_x = U_m x/\nu$, depending on the rotation rate and the main flow Reynolds number $Re = U_m d/\nu$. It suggests that Reynolds number Re_x may not be an appropriate parameter to predict the boundary layer transition. Using the data in Fig. 11, the shape

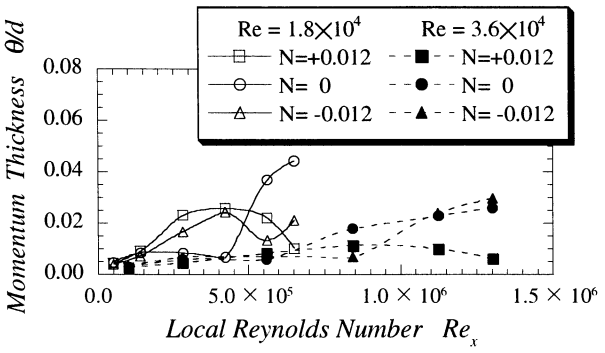

(a) Momentum thickness

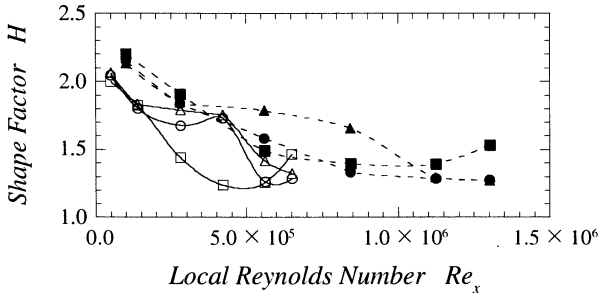

(b) Shape factor

Fig.11 Changes in momentum thickness and shape factor along the concave wall of R = 2,000mm

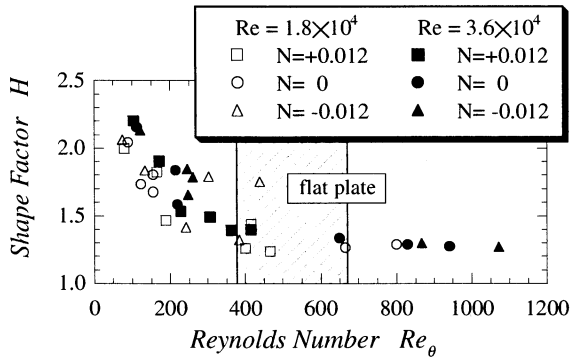

Fig.12 Relation between Re_θ and H

factor, H, is plotted against the Reynolds number based on the momentum thickness, $Re_\theta = U_m\theta/\nu$, as shown in Fig. 12. It is seen that the transition occurs at the point where Re_θ exceeds 400, irrespective of the difference in the axial Reynolds number, Re, rotation rate, N or curvature radius of the wall, R. This critical Reynolds number almost agrees with that obtained on a flat plate in the stationary state($Re_{\theta cr}$ = 376～664) as shown in the same figure.

4. Conclusions

The velocity and turbulence intensity in the boundary layer near the concave wall were measured for different rotation rates and the effects of the Coriolis and centrifugal forces are examined experimentally. The results of the present study can be summarized as follows;

(1) The Coriolis force exerted normally toward the wall promotes the Görtler instability and advances the transition of the boundary layer flow from laminar to turbulent state, but that exerted away from the wall delays the transition.

(2) The transition occurs when the Reynolds number based on the momentum thickness exceeds a critical value, regardless of the difference in the rotation rate and the main flow velocity.

(3) At negative rotation rates the fluctuating component is suppressed and a further decrease generates a different type of instability to the boundary layer flow.

References

Bradshaw, P., 1969, "The Analogy between Streamline Curvature and Buoyancy in Turbulent Shear Flow", *Journal of Fluid Mechanics*, 36, 177-191,

Kikuyama, K., Nishibori, K., Hara, S., 1987, "Effects of System Rotation upon Turbulent Boundary Layer on a Concave Surface", *Proc. 6th Sympo. on Turbulent Shear Flows*, 1.4.1

Kikuyama, K., Hasegawa, Y., Yokoi, T., and Hirota, M., 1994, "Effects of Coriolis Force on Instability of Laminar Boundary Layer on a Concave Surface", ASME *Gas Turbine Conference*, Paper 94-GT-287, 1-8.

Kikuyama K., Hasegawa, Y., and Ooe, T., 2000, "Effects of Channel Rotation and Wall Curvature on T-S Instability", *Proc. 3rd Int. Sympo. on Turbulent, Heat and Mass Transfer*, 669-676.

Koyama, H., Masuda, S., Ariga, I., and Watanabe, I., 1979, "Stabilizing and Destabilizing Effects of Coriolis Force on Two-dimensional Laminar and Turbulent Boundary Layers",, Trans. ASME, *J. Engng. Power*, Vol.101, pp. 23-31

Matsson, O. J. E., and Alfredsson, P. H., 1990, "Curvature- and Rotation-Induced Instabilities in Channel Flow", *Journal of Fluid Mechanics*., Vol. 210, p.537.

Matsubara, M., and Masuda, S., 1991, "Three-dimensional Instability in Rotating Boundary Layer", FED-Vol.114, Boundary layer Stability and Transition to Turbulence, ASME, pp. 103-107.

Nomenclature

d : Width of cross-section (mm)
h : Height of cross-section (mm)
H : Shape factor of boundary layer
N : Rotation rate (Eq.(1))
R : Radius of curvature for channel center-line (mm)
Re : Axial Reynolds number = $U_m d/\nu$
Re_x : Local Reynolds number = $U_m x/\nu$
Re_θ : Reynolds number based on momentum thickness = $U_m\theta/\nu$
u' : Rms value of fluctuating velocity component (m/s)
U_m : Free stream velocity at O_1 section (m/s)
U_{max}: Free stream velocity at each section (m/s)
Ω : Rotational speed of channel (1/sec)
θ : Momentum thickness of boundary layer (mm)